The Equilibrium Unfolding Intermediate Observed at pH 4 and its Relationship with the Kinetic Folding Intermediates in Green Fluorescent Protein

ARTICLE *in* JOURNAL OF MOLECULAR BIOLOGY · OCTOBER 2006

Impact Factor: 4.33 · DOI: 10.1016/j.jmb.2006.07.009 · Source: PubMed

9 AUTHORS, INCLUDING:

Kosuke Maki
Nagoya University
45 PUBLICATIONS **1,266** CITATIONS
SEE PROFILE

Tomonao Inobe
University of Toyama
31 PUBLICATIONS **502** CITATIONS
SEE PROFILE

Tomotaka Oroguchi
Keio University
31 PUBLICATIONS **195** CITATIONS
SEE PROFILE

Kunihiro Kuwajima
The University of Tokyo
157 PUBLICATIONS **7,598** CITATIONS
SEE PROFILE

doi:10.1016/j.jmb.2006.07.009 J. Mol. Biol. (2006) 361, 969–982

JMB

Available online at www.sciencedirect.com

ScienceDirect

ELSEVIER

The Equilibrium Unfolding Intermediate Observed at pH 4 and its Relationship with the Kinetic Folding Intermediates in Green Fluorescent Protein

Sawako Enoki, Kosuke Maki, Tomonao Inobe, Kazunobu Takahashi Kiyoto Kamagata, Tomotaka Oroguchi, Hiroyasu Nakatani Katsuaki Tomoyori and Kunihiro Kuwajima*

Department of Physics Graduate School of Science University of Tokyo, 7-3-1 Hongo, Bunkyo-ku Tokyo 113-0033, Japan

**Corresponding author*

Folding mechanisms of a variant of green fluorescent protein (F99S/M153T/V163A) were investigated by a wide variety of spectroscopic techniques. Equilibrium measurements on acid-induced denaturation of the protein monitored by chromophore and tryptophan fluorescence and small-angle X-ray scattering revealed that this protein accumulates at least two equilibrium intermediates, a native-like intermediate and an unfolding intermediate, the latter of which exhibits the characteristics of the molten globule state under moderately denaturing conditions at pH 4. To elucidate the role of the equilibrium unfolding intermediate in folding, a series of kinetic refolding experiments with various combinations of initial and final pH values, including pH 7.5 (the native condition), pH 4.0 (the moderately denaturing condition where the unfolding intermediate is accumulated), and pH 2.0 (the acid-denaturing condition) were carried out by monitoring chromophore and tryptophan fluorescence. Kinetic on-pathway intermediates were accumulated during the folding on the refolding reaction from pH 2.0 to 7.5. However, the signal change corresponding to the conversion from the acid-denatured to the kinetic intermediate states was significantly reduced on the refolding reaction from pH 4.0 to pH 7.5, whereas only the signal change corresponding to the above conversion was observed on the refolding reaction from pH 2.0 to pH 4.0. These results indicate that the equilibrium unfolding intermediate is composed of an ensemble of the folding intermediate species accumulated during the folding reaction, and thus support a hierarchical model of protein folding.

Keywords: protein folding; molten globule state; folding intermediate; green fluorescent protein; X-ray scattering

Introduction

Green fluorescent protein (GFP) from the jellyfish *Aequorea victoria* is a soluble globular protein consisting of 238 residues. GFP is a large single domain protein (27 kDa) and has a *p*-hydroxybenzylideneimidazolidone chromophore that emits green fluorescence (Figure 1).[1,2] The chromophore is formed by autocatalytic cyclization of a polypeptide backbone of Ser65, Tyr66, and Gly67.[3–5] Eleven β-strands make a large β-can structure of GFP, and the chromophore is located at the center of the β-can. The chromophore is shielded from the bulk water molecules by the surrounding β-strands and capping α-helices, and GFP has an extensive

Present addresses: S. Enoki, The Institute of Scientific and Industrial Research, Osaka University, Ibaraki, Osaka 567-0047, Japan; T. Inobe, Department of Biochemistry, Molecular Biology and Cell Biology, Northwestern University, 2205 Tech Drive, Evanston, IL 60208, USA; K. Kamagata, Institute for Protein Research, Osaka University, Suita, Osaka 565-0871, Japan.

Abbreviations used: D, denatured state; GFP, green fluorescent protein; GFPuv, a mutant (F99S/M153T/V163A) of green fluorescent protein; I, intermediate state; N, native state; SAXS, small-angle X-ray scattering; R_g, radius of gyration; SVD, singular value decomposition.

E-mail address of the corresponding author: kuwajima@gagliano.phys.s.u-tokyo.ac.jp

0022-2836/$ - see front matter © 2006 Elsevier Ltd. All rights reserved.

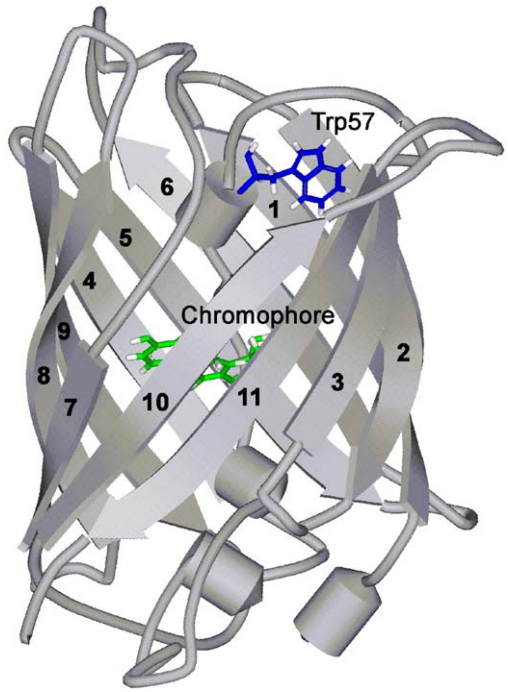

Figure 1. Schematic representations of the backbone structure of a GFP mutant, GFPuv (PDB code: 1b9c) drawn using DS Modeling. The chromophore and Trp57 are shown as ball-and-stick model. The number is labeled for each β-strand from the N to C termini.

hydrogen bond network around the chromophore. Although initial folding studies of GFP were reported as early as the 1980s,[6,7] a quantitative analysis of fast refolding reactions of GFP has been published only recently.[8]

Investigation of the folding mechanism of GFP is important for three major reasons. (1) Because of its specific green fluorescence in the native state, GFP is a useful model for studying protein folding in a complex environment with molecular chaperons and other molecules such as those in the biological cell.[9–12] The study of *in vitro* folding of GFP will thus provide a basis for such studies of GFP folding in the complex environment. (2) GFP is used widely as a marker of protein expression and localization in the field of molecular cell biology[13] and hence it is important to investigate the physicochemical properties of GFP itself. (3) GFP has a peculiar backbone topology (β-can fold), which shows remarkably high values of backbone topological parameters, such as absolute contact order (*ACO*) and the number of sequence-distant native pairs (Q_d), as compared with the corresponding parameter values of other globular proteins; the *ACO* and Q_d values of GFP are 29.5 and 214, respectively, which are both the highest among for 40 globular proteins investigated.[14] Because the backbone topological parameters are known to be closely related to the folding mechanism of globular proteins, the folding reaction of GFP itself is thus intriguing.

We previously studied the kinetic refolding of a mutant (F99S/M153T/V163A) of GFP (GFPuv; also known as the Cycle3 mutant) from the acid-denatured state by stopped-flow fluorescence and stopped-flow circular dichroism (CD) spectroscopy. The structure and folding behavior of the mutant are known to be essentially identical to those of the wild-type protein, while the reversibility of unfolding is much better for the mutant than for the wild-type.[15,16] It has been shown that the kinetics of the refolding of the protein have at least five kinetic phases, and involve non-specific collapse within the dead time of a stopped-flow apparatus and the subsequent formation of an on-pathway intermediate with the characteristics of the molten globule state.[8] The slowest phase and a major portion of the second slowest phase were also found to be rate-limited by slow prolyl isomerization in the intermediate states. However, the detailed characteristics of the kinetic folding intermediate of the protein have not yet been well characterized because such intermediates are populated only transiently during the kinetics.

The kinetic folding intermediate of a number of globular proteins, including apomyoglobin, ribonuclease HI, and α-lactalbumin, is known to be equivalent to the equilibrium unfolding intermediate populated under a mildly denaturing condition.[17–24] To elucidate the mechanism of protein folding, it is therefore often useful to investigate the equilibrium unfolding intermediate instead of the kinetic folding intermediate. To date, detailed characterization of the folding intermediate has been carried out only in a small number of globular proteins, and it is important to characterize the intermediates of proteins with different backbone topologies.

Here, we investigated the acid denaturation of GFPuv (the mutant F99S/M153T/V163A) by chromophore fluorescence, tryptophan fluorescence, and small-angle X-ray scattering (SAXS). We show that the equilibrium unfolding intermediate of GFPuv is populated under a mildly acidic condition (pH 4.0). We characterized the intermediate in detail and investigated the relationship between the kinetic folding intermediates and the equilibrium unfolding intermediate. The kinetic intermediate of GFPuv is shown to be equivalent to the equilibrium intermediate populated at pH 4.0. Finally, we discuss the folding mechanism of GFPuv in comparison with those of other globular proteins that exhibit the molten globule folding intermediate.

Results

Tryptophan fluorescence spectra

Figure 2 shows tryptophan fluorescence spectra of GFPuv excited at 295 nm at various pH values at 0.04 mg/ml of the protein. We also measured the spectra at a higher concentration (0.5 mg/ml) of GFPuv, and obtained essentially the same results. The spectra may provide information regarding the

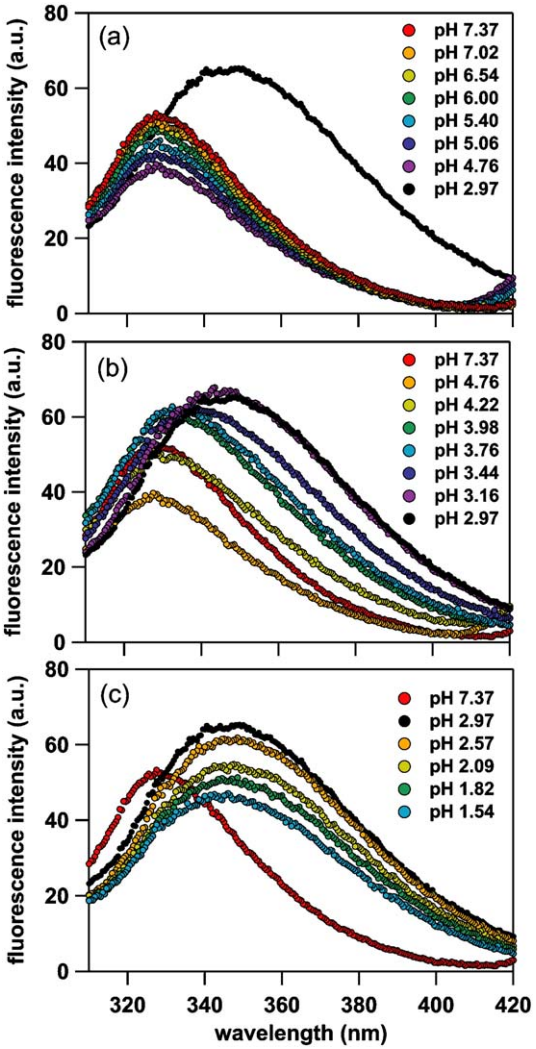

Figure 2. Tryptophan fluorescence spectra of GFPuv excited at 295 nm at various pH values. (a) pH 7.37–pH 4.76, (b) pH 4.76–pH 2.97, and (c) pH 2.97–pH 1.54. Red and black circles in each panel show the fluorescence spectra of the native state at pH 7.37 and the acid-denatured state at pH 2.97, respectively. The protein concentration was 0.04 mg/ml.

environment around Trp57, because this is the only tryptophan residue of GFPuv. From Figure 2, there are four typical pH regions regarding tryptophan fluorescence spectral changes: (1) From pH 1.5 to pH 3, the fluorescence peak is located at 347 nm and the fluorescence intensity increases; (2) from pH 3 to pH 4, the fluorescence peak is shifted from 347 nm to 334 nm with a slight decrease in the fluorescence intensity; (3) from pH 4 to pH 4.8, the fluorescence peak is shifted from 334 nm to 330 nm and the fluorescence intensity decreases, and (4) from pH 4.8 to pH 7.5, there is no peak shift but the fluorescence intensity increases.

The tryptophan fluorescence peak position is plotted as a function of pH in Figure 4(a), below. The peak position may be used as an indicator of the polarity of the environment of the tryptophan residue.[25] We have also plotted the integral intensity of tryptophan fluorescence in a region for the native state (325 nm–335 nm) and that for the acid-denatured state (342 nm–352 nm) in Figure 4(b), below. These spectra were measured 6–9 h after the unfolding started, as the spectral change was saturated at 6 h, and no further change was observed after the saturation.

Small-angle X-ray scattering

Figure 3 shows scattering curves of GFPuv measured by SAXS at various pH values, and here the scattering intensity I is shown as a function of a momentum transfer Q, which is given by $Q=(4\pi \sin\theta)/\lambda$ (λ, wavelength; and 2θ, scattering angle). The protein concentration for each curve is 0.5 mg/ml. The scattering curves were measured more than 4 h after the unfolding was started, except for the curve at pH 2.2, where the unfolding time was only 1 h. These unfolding times are enough for the saturation of the acid-induced change in the scattering curve, and the scattering curves measured after longer unfolding times, 10 h at pH 4.0 and 12 h at pH 2.2, were essentially identical to the curves after the saturation.

We used the integral scattering intensity in a region of Q from 0.045 Å^{-1} to 0.12 Å^{-1} to monitor the unfolding, and the transition curve given by the integral scattering intensity as a function of pH is shown in Figure 4(c). The scattering curve at pH 4.5 increases in a small angle region ($Q<0.04$ Å^{-1}), suggesting the presence of protein aggregation. The

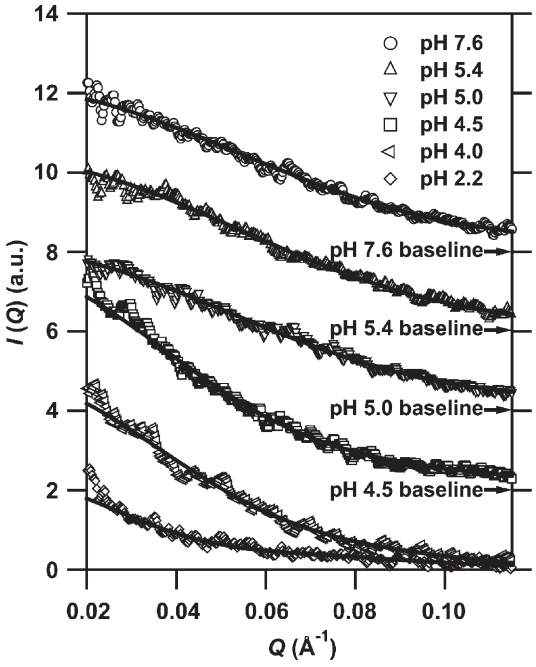

Figure 3. The X-ray scattering curves of GFPuv at various pH values. The continuous lines show the theoretical curves calculated from the individual $P(r)$ profiles in Figure 5 using the GNOM program.[27] The baselines of the scattering curves at pH 7.6, pH 5.4, pH 5.0, and pH 4.5 are shifted for clarity, which are shown by arrows. The protein concentration was 0.5 mg/ml.

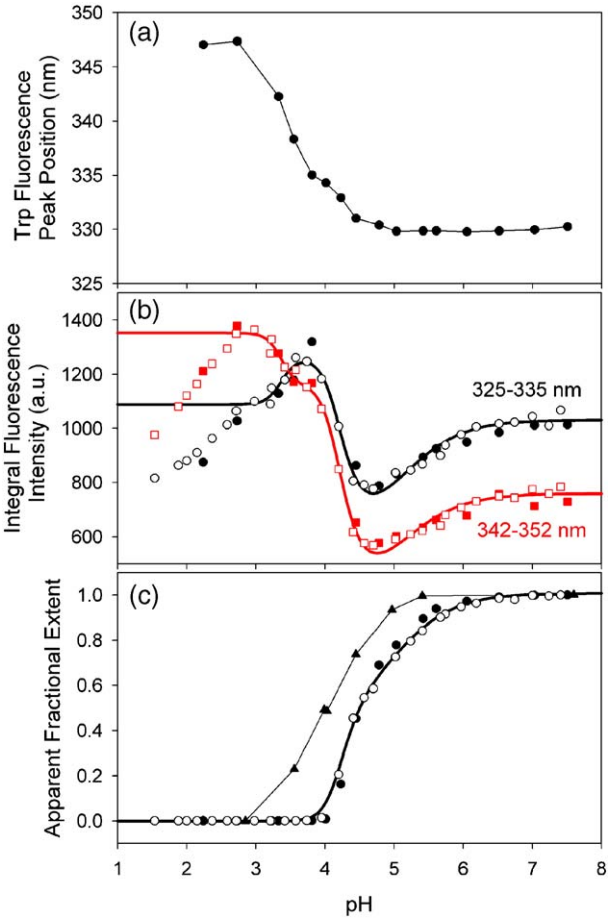

Figure 4. Acid-induced denaturation of GFPuv under equilibrium conditions monitored by various probes. (a) Tryptophan fluorescence peak positions excited at 295 nm; (b) integral intensity of tryptophan fluorescence around the peak positions of the native state at pH 7.6 (325 nm–335 nm) (open and filled circles) and that of the acid-denatured state at pH 2.2 (342 nm–352 nm) (open and filled squares (red)); (c) normalized integral SAXS intensity ($0.045\ \text{Å}^{-1} < Q < 0.118\ \text{Å}^{-1}$) (filled triangles) and normalized chromophore fluorescence intensity (open and filled circles), where the intensities for the denatured state and the native state are 0 and 1, respectively. The protein concentrations used were 0.04 mg/ml (open symbols) and 0.5 mg/ml (filled symbols).

aggregation of the protein is likely to occur most significantly at pH 4.5 because of its isoelectric point at pH 5. Although even a small aggregation fraction affects the scattering curve in a small angle region ($Q < 0.04\ \text{Å}^{-1}$), the effect of the aggregation on the scattering curve in a region of Q from $0.045\ \text{Å}^{-1}$ to $0.12\ \text{Å}^{-1}$ is small.

Fluorescence spectra of the green fluorescent chromophore

The fluorescence spectrum of the *p*-hydroxybenzylideneimidazolidone chromophore of GFPuv with excitation at 395 nm was measured as a function of pH. In contrast to the tryptophan fluorescence of the protein shown above, the chromophore fluorescence was observed only above pH 4.0, and there was neither a peak shift nor a change in the spectral shape during the transition.[8] Only the spectral intensity is changed by the unfolding transition. Chromophore fluorescence can be emitted only in the native state, because the specific native structure around the chromophore is required for the fluorescence emission.

Figure 4(c) shows the acid-induced unfolding transition of GFPuv measured by chromophore fluorescence intensity at 508 nm. The measurements were carried out under the same conditions as used in SAXS measurements and tryptophan fluorescence spectral measurements. The chromophore fluorescence increases sharply from pH 4.0 to pH 4.8 and then increases slightly above pH 4.8. The fluorescence spectra were measured 6 to 8 h after the unfolding of GFPuv started.

Acid-induced Unfolding Transition

Transition curves

From comparisons of the transition curves measured by different structural probes (Figure 4), it is clear that the acid-induced unfolding of GFPuv is not a two-state transition. The transition curves measured by SAXS and tryptophan fluorescence do not coincide with that measured by chromophore fluorescence. Although the unfolding of GFPuv is not fully reversible, the unfolding conditions, including the protein concentration (0.5 mg/ml), temperature (25 °C), and buffer compositions, were the same throughout the present experiments (Figure 4), indicating that the two-state transition must give a coincident transition curve. Furthermore, the transition curves measured by tryptophan fluorescence and chromophore fluorescence were obtained at two different concentrations (0.04 and 0.5 mg/ml) of the protein, and they are coincident with each other (Figure 4(b) and (c)).

The four typical pH regions for the acid transition of GFPuv mentioned above are further characterized by the transition curves of Figure 4. (1) From pH 1.5 to pH 3, the tryptophan fluorescence peak is located at 347 nm with an increase in the fluorescence intensity, and the chromophore fluorescence and the SAXS results indicate that the protein is still fully acid-denatured. (2) From pH 3 to pH 4, the tryptophan fluorescence peak is shifted to a shorter wavelength with a slight decrease in the intensity, but the green fluorescent chromophore does not emit any fluorescence. According to the SAXS results, some overall compact structure is formed at pH 4.0 (see below), and hence the transition from pH 3 to pH 4 may correspond to accumulation of an intermediate that does not have chromophore fluorescence but that is compact compared with the acid-denatured state. (3) From pH 4 to pH 4.8, the tryptophan fluorescence peak is shifted to an even shorter wavelength with a decrease in the

fluorescence intensity, and the chromophore fluorescence increases sharply. (4) From pH 4.8 to pH 7.5, there is no tryptophan fluorescence peak shift, but the intensities of tryptophan fluorescence and chromophore fluorescence increases. The overall structure measured by SAXS is native-like in this pH region (see below).

Modeling of the acid-induced unfolding

From the unfolding transition curves in Figure 4, there are at least three transitions: (1) from the native state (N) to the native-like intermediate (N′) that is accumulated at pH 4.8; (2) from N′ to the compact unfolding intermediate (I) that is accumulated at pH 4; and (3) from I to the acid-denatured state (D) that is stable below pH 3. We therefore model the acid-induced unfolding of GFPuv with a simple sequential four-state model as:

$$\mathrm{N} \overset{K_{\mathrm{NN'}}}{\rightleftharpoons} \mathrm{N'} \overset{K_{\mathrm{NI}}}{\rightleftharpoons} \mathrm{I} \overset{K_{\mathrm{ID}}}{\rightleftharpoons} \mathrm{D}, \qquad \text{Scheme 1}$$

where $K_{\mathrm{NN'}}$, $K_{\mathrm{N'I}}$, and K_{ID} are the equilibrium constants between N and N′, between N′ and I, and between I and D, respectively. The pH dependence of these equilibrium constants is related to the pK_a values of ionizable groups that are associated with the transition as:[26]

$$K_{\mathrm{ij}}(\mathrm{pH}) = K_{\mathrm{ij}}^{\circ}\left(\frac{1+10^{\mathrm{p}K_{\mathrm{aj}}/10^{\mathrm{pH}}}}{1+10^{\mathrm{p}K_{\mathrm{ai}}/10^{\mathrm{pH}}}}\right)^{n_{\mathrm{ij}}}, \qquad (1)$$

where i and j stand for the states (N, N′, I or D) before and after the transition, pK_{ai} and pK_{aj} are the pK_a values of the ionizable groups in state i and state j, respectively, and n_{ij} is the number of ionizable groups associated with the transition from i to j. For simplicity, here we have assumed that the ionizable groups have the same pK_{ai} and the same pK_{aj} values when there are more than one ionizable group associated.

We analyzed the unfolding transition curves measured by the tryptophan integral fluorescence intensities between 325 nm and 335 nm and between 342 nm and 352 nm (Figure 4(b)) and by the chromophore fluorescence intensity at 508 nm (Figure 4(c)) on the basis of equation (1). With equation (1), the pH dependence of the observed fluorescence intensity F_{obs} is represented by:

$$F_{\mathrm{obs}} = \frac{F_{\mathrm{N}} + F_{\mathrm{N'}}K_{\mathrm{NN'}} + F_{\mathrm{I}}K_{\mathrm{NN'}}K_{\mathrm{N'I}} + F_{\mathrm{D}}K_{\mathrm{NN'}}K_{\mathrm{N'I}}K_{\mathrm{ID}}}{1 + K_{\mathrm{NN'}} + K_{\mathrm{NN'}}K_{\mathrm{N'I}} + K_{\mathrm{NN'}}K_{\mathrm{N'I}}K_{\mathrm{ID}}} \qquad (2)$$

where F_{N}, $F_{\mathrm{N'}}$, F_{I}, and F_{D} are the fluorescence intensities of the pure N, N′, I, and D states, respectively. We performed non-linear least-squares global fitting for the three unfolding transition curves measured by the fluorescence intensities (Figure 4(b) and (c)). There are 24 fitting parameters, i.e., K_{ij}°, pK_{ai}, pK_{aj}, and n_{ij} for each of the three transitions, which result in 12 global parameters, and F_{N}, $F_{\mathrm{N'}}$, F_{I}, and F_{D} for each of the three transition curves, which result in 12 local parameters. We have assumed that these parameters are independent of pH and that n_{ij} is a positive integer. For the tryptophan integral fluorescence intensities (Figure 4(b)), we used the data between pH 2.9 and pH 7.5 for the analysis, because the fluorescence change below pH 2.9 cannot be ascribed to ionization of ionizable groups in protein. The best-fit parameter values for n_{ij}, K_{ij}°, pK_{ai}, and pK_{aj} for the three transitions are summarized in Table 1. In general, the pK_{ai} value that is an abnormal pK_a value before the transition cannot be determined uniquely, and hence only upper limits are shown (Table 1). Because the unfolding transition of GFPuv is not fully reversible[8] the parameter values shown in Table 1 may be regarded as semi-quantitative.

From Table 1, the NN′ transition is associated with ionization of a group that has a pK_{aN} less than 4.5 and a p$K_{\mathrm{aN'}}$ of 6.6, and this is identified as a histidine. The N′I transition is associated with ionization of five groups that have a p$K_{\mathrm{aN'}}$ less than 2.5 and a pK_{aI} of 4.3, and these groups are identified as carboxyls (glutamyl and aspartyl groups). The ID transition is associated with ionization of five groups that have a pK_{aI} less than 2.5 and a pK_{aD} of 4.1. These groups are also identified as carboxyls, but the pK_{aD} value is closer to those of aspartyl and α-carboxyl groups. Thick continuous lines in Figure 4(b) and (c) are the theoretical curves drawn using these parameter values. The theoretical curves show excellent agreement with the experimental data except for those below pH 2.9 in Figure 4(b), which were not used in the least-squares fitting. The tryptophan integral fluorescence intensities decrease with decreasing pH below pH 2.9, and this decrease in the intensity may be caused by ionic-strength effect and/or anion (Cl^-) binding, because we used HCl to adjust pH in this region.

SAXS analysis

To further characterize the structure of GFPuv in the native, intermediate, and acid-denatured states in solution, we further analyzed the X-ray scattering curves to obtain the pair-distance distribution ($P(r)$) functions, which gave us estimates of the maximum distance D_{max} and the radius of gyration R_{g} of GFPuv in each state. To test the validity of the four-state equilibrium unfolding model (Scheme 1), we

Table 1. n_{ij}, K_{ij}°, pK_{ai}, and pK_{aj} values used in fitting the transition curves measured by the fluorescence intensities (Figure 4(b) and (c)) of GFPuv

Ionizable groups	Transition		pK_{ai} or pK_{aj}			
	n_{ij}	K_{ij}°	pK_{aN}	p$K_{\mathrm{aN'}}$	pK_{aI}	pK_{aD}
Histidine	N ⇌ N′ $n_{\mathrm{NN'}}=1$	$K_{\mathrm{NN'}}^{\circ}=2.7\times10^{-2}$	<4.5	6.6	6.6	6.6
Carboxyls	N′ ⇌ I $n_{\mathrm{N'I}}=5$	$K_{\mathrm{N'I}}^{\circ}=3.2\times10^{-2}$	<2.5	<2.5	4.3	4.3
Carboxyls	I ⇌ D $n_{\mathrm{ID}}=5$	$K_{\mathrm{ID}}^{\circ}=1.7\times10^{-4}$	<2.5	<2.5	<2.5	4.1

also applied the singular value decomposition (SVD) to a series of the X-ray scattering curves.

Pair-distance distribution functions

Figure 5 shows $P(r)$ functions of GFPuv at pH 7.6 (the N state), pH 5.4, pH 5.0 (the N′ state), pH 4.5, pH 4.0 (the I state), and pH 2.2 (the D state). The $P(r)$ functions, which were obtained by an indirect Fourier transformation method using the GNOM program,[27] represent the distributions of distances between all pairs of atoms of the scatterer, and hence give us information about the size and shape of the scatterer molecule. The Q region used to calculate the $P(r)$ function did not include the small angle region where the effect of the aggregation was observed. The region used for calculating the $P(r)$ function is shown in the legend of Figure 5. We also obtained the X-ray scattering curves predicted from the individual $P(r)$ profiles, and continuous lines in Figure 3 show these predicted scattering curves. GFPuv at pH 7.6, 5.4 and 5.0 has a native globular structure, and the $P(r)$ function of GFPuv at pH 5.0 is almost the same as that at pH 7.6, but shifted slightly to a longer distance distribution. Therefore, the N and N′ states are very similar to each other in the overall shape, but N′ is slightly expanded.

The maximum distance D_{max} of the $P(r)$ function in the N state, given by an intercept on the r-axis, is 62 Å, and this is a little larger than the D_{max} (55 Å) calculated from the X-ray crystallographic structure of GFPuv (PDB code: 1b9c). This difference of D_{max} may be due to the absence of ten amino acid residues in the X-ray crystallographic structure as well as to the presence of hydration water molecules on the surface of the GFPuv molecule in solution. GFPuv in the D state at pH 2.2 has a broad distribution with two peaks, indicating that GFPuv at this pH has an expanded structure but that the structure is not fully unfolded. This result is consistent with the far-UV CD spectral data in a previous study, which has shown that the acid-denatured state at pH 2.0 is not fully unfolded but has, to an extent, a secondary structure.[8] The $P(r)$ function of GFPuv at pH 4.0, where the I state accumulates, shows a peak at 35 Å with a shoulder, and the D_{max} of the $P(r)$ function is 92 Å. This may indicate that the I state has a molten globule-like structure resulting from a hydrophobic core with flaring tails.[28] It might also be possible that the shoulder of the $P(r)$ function is due to a small fraction of protein aggregation. The apparent extent of unfolding measured by the SAXS intensity is only 0.5, and there is no plateau at pH 4.0 in the transition curve (Figure 4(c)).

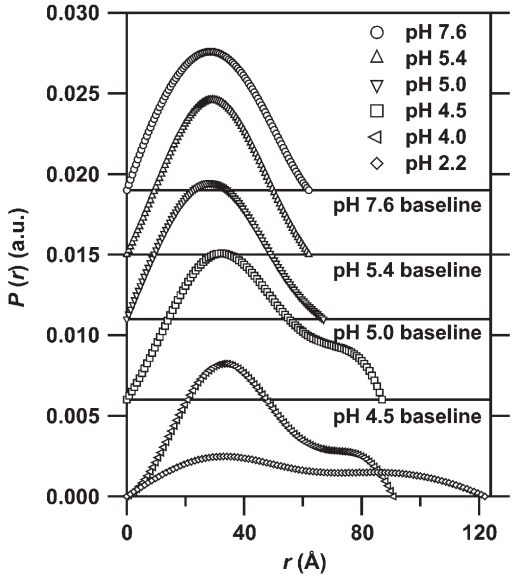

Figure 5. Pair distribution function, $P(r)$, of GFPuv at various pH values. The $P(r)$ profiles were calculated from the SAXS patterns shown in Figure 3. The baselines of the $P(r)$ functions at pH 7.6, pH 5.4, pH 5.0, and pH 4.5 are shifted for clarity and explicitly shown by continuous lines. For the calculation, the used maximum Q was 0.118 Å^{-1}, and the used minimum Q were 0.032 Å^{-1} (pH 7.6), 0.027 Å^{-1} (pH 5.4), 0.021 Å^{-1} (pH 5.0), 0.035 Å^{-1} (pH 4.5), 0.029 Å^{-1} (pH 4.0), and 0.025 Å^{-1} (pH 2.2). The D_{max} values were 62 Å (pH 7.6), 62 Å (pH 5.4), 67 Å (pH 5.0), 87 Å (pH 4.5), 91 Å (pH 4.0), and 122 Å (pH 2.2).

The R_g values were computed from the $P(r)$ functions using GNOM. The R_g values of GFPuv at pH 7.6 (the N state), at pH 2.2 (the D state), and at pH 4.0 (the I state) are 22.9 Å, 43.8 Å, and 32.3 Å, respectively. The R_g in the N state at infinite dilution without the inter-particle interference was also obtained by extrapolating the observed R_g to zero protein concentration by the plot of R_g^2 *versus* protein concentration (data not shown), and the R_g value thus obtained was 20.8 Å. The R_g value in the N state is thus larger than that calculated from the X-ray structure (16.6 Å). The difference in R_g is probably again due to the absence of ten amino acid residues located at the C and N termini of GFPuv in the crystal structure as well as to the hydration effect. The presence of the dimer state may be excluded as a cause of the difference, because the D_{max} value of native GFPuv is slightly larger but agrees reasonably with that calculated from the crystal structure.

The R_g value in the D state was found to be significantly smaller than the R_g value expected for the fully unfolded polypeptide of GFPuv (50.8 Å), which was estimated by a power-law relationship between a polymer length and an ensemble averaged R_g obtained by Kohn *et al.*[29] further indicating the incomplete unfolding of the D state.

Singular value decomposition (SVD)

We carried out the SVD of a series of X-ray scattering curves of GFPuv at various pH values from pH 7.6 to pH 2.2.[30,31] The first three components from the SVD clearly exhibit signals that represent the transition behavior, and they have the following singular values: $s_1 = 138.53$ (contribution 80.7%), $s_2 = 14.90$ (8.7%), and $s_3 = 4.84$ (2.8%). Figure 6(a), (b) and (c) show the basis scattering curves of these first three components, and Figure 6(d), (e) and (f)

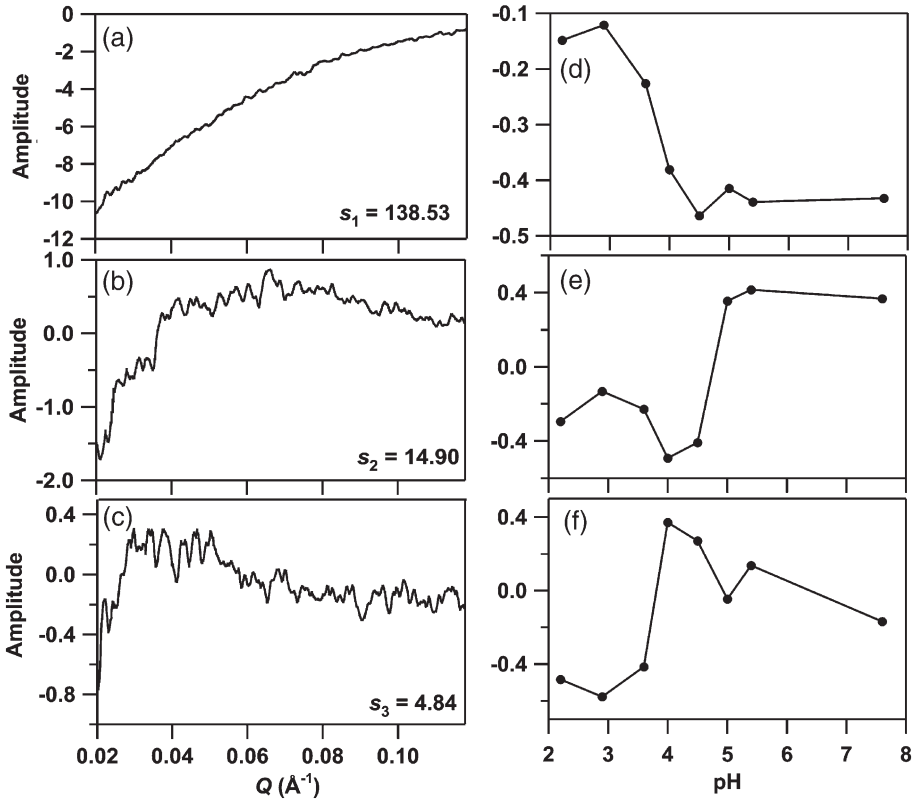

Figure 6. The basis scattering curves ((a)–(c)) and the corresponding pH-dependent amplitudes ((d)–(f)) obtained by the SVD of the X-ray scattering profiles of GFPuv at various pH values. The first three singular values were: $s_1 = 138.53$, $s_2 = 14.90$, $s_3 = 4.84$.

show the pH profiles of the corresponding amplitudes. Although the apparent transition curve measured by the integral SAXS intensity in Figure 4(c) cannot discriminate between different transitions, the pH profiles of the amplitudes of the SVD components clearly show the presence of at least two acid-induced transitions of GFPuv. The amplitude of the first component exhibits a transition between pH 4 and pH 3, and this corresponds to the ID transition observed by the tryptophan fluorescence (Figure 4(b)). The ID transition is also seen in the pH profiles of the second and third components. The pH profiles of the second and third components also show a transition between pH 5 and pH 4, and this may correspond to the N′I transition observed by the tryptophan and chromophore fluorescence (Figure 4(b) and (c)). However, the transition measured by the SVD components apparently occurs at a higher pH, and this behavior is probably due to aggregation of the protein, because GFPuv tends to aggregate in this pH region, especially at a high concentration (0.5 mg/ml) used in the SAXS experiments. The NN′ transition observed by the tryptophan and chromophore fluorescence (Figure 4(b)) cannot be seen clearly in the pH profiles of the SVD components. This is reasonable because the SAXS pattern of GFPuv is almost the same between N and N′. The above results of the SVD are thus fully consistent with the four-state equilibrium unfolding model shown above (Scheme 1).

Kinetic refolding reactions from the acid-denatured state (pH 2.0) and from the equilibrium intermediate (pH 4.0) to the native state (pH 7.5)

To investigate the relationship between the kinetic folding intermediates and the equilibrium intermediate (I) accumulated at pH 4.0 we measured the kinetic refolding reactions induced by pH jumps from acidic pH values (pH 2.0 and pH 4.0) to pH 7.5 by monitoring the chromophore fluorescence and the tryptophan fluorescence.

Figure 7(a) shows the kinetic refolding reactions induced by pH jumps from pH 2.0 and pH 4.0 to pH 7.5 as monitored by the fluorescence of the GFPuv chromophore. Both refolding curves of GFPuv were fitted with four exponentials with the same four rate constants. The resultant kinetic parameters are summarized in Table 2. In both the refolding curves, the sign of the amplitude of the fastest observable phase was opposite to the sign of the subsequent slower phases, suggesting that this phase is a lag phase caused by the accumulation of an on-pathway folding intermediate; this phase corresponds to the second phase in the kinetics measured by the tryptophan fluorescence (see below). However, the amplitude of this second phase (lag phase) of GFPuv refolding from pH 4.0 was reduced to 65% of the amplitude of refolding from pH 2.0. The subsequent slower phases of refolding from pH 4.0 were essentially the same as those of refolding from pH

2.0. The refolded GFPuv after denaturing at pH 4.0 and pH 2.0 each restored 90% of the native fluorescence, indicating that there was no difference in reversibility between the two refolding reactions from the different pH values.

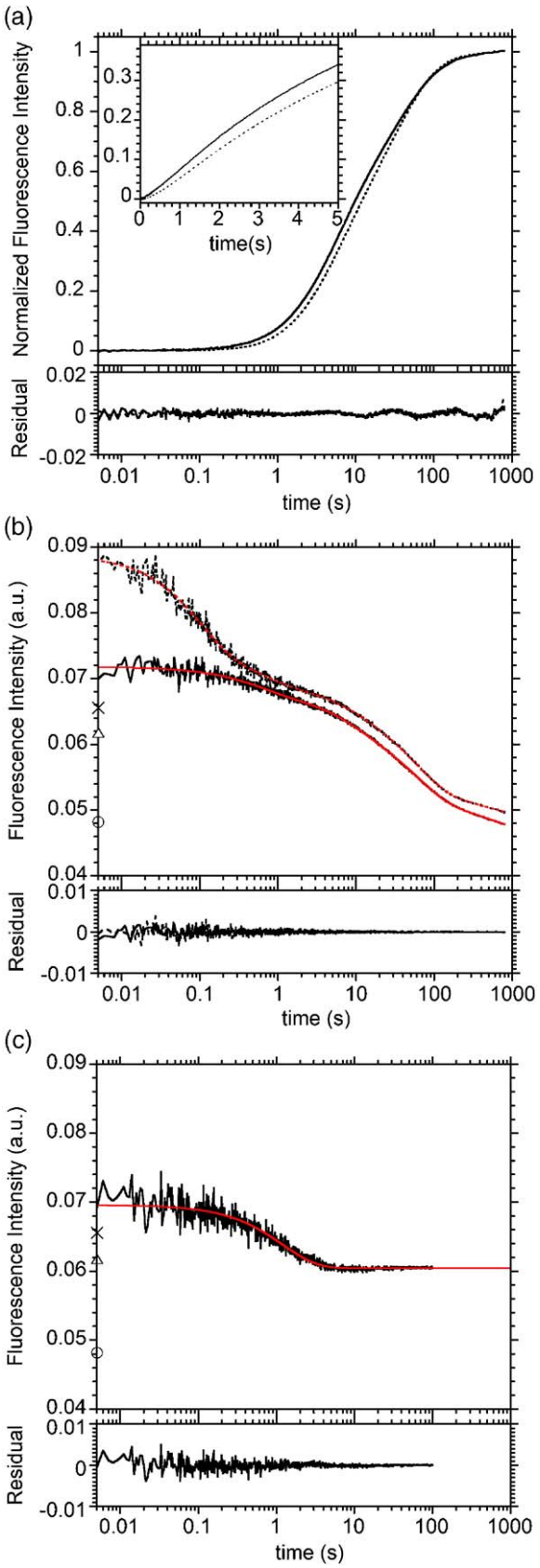

Figure 7(b) shows refolding curves monitored by tryptophan fluorescence excited at 295 nm. The refolding was initiated by pH jumps from pH 2.0 (dotted line) and pH 4.0 (continuous line) to pH 7.5. There was a burst phase, occurring within the dead time (5 ms) of the stopped-flow measurement, in each refolding reaction. We can fit the observable kinetics after the burst phase with five exponentials with the same five rate constants for the two refolding reactions. The relative amplitudes in the following are set at 0% for the D state and 100% for the N state. When the refolding reaction was initiated from pH 2.0, the fluorescence intensity increased largely (−134%) in the burst phase. Because tryptophan fluorescence is quenched by the green fluorescent chromophore in native GFPuv, the positive amplitude percent indicates a decrease in tryptophan fluorescence intensity, and hence the relative amplitude of −134% indicates an increase in the fluorescence intensity. When the refolding reaction was initiated from pH 4.0, the fluorescence again increased in the burst phase, but the amplitude (−35.3%) of the fluorescence change decreased remarkably as compared with that in the refolding initiated from pH 2.0. The burst-phase increase of the tryptophan fluorescence in the refolding from pH 2.0 to pH 7.5 may partly arise from the ionic strength and/or the anion-binding effects that we have seen in the transition curves below pH 2.9 (Figure 4(b)). However, our previous study has shown that this burst-phase is also observed in the presence of 0.1 M NaCl[8] and hence it may arise mainly from a rapid collapse in GFPuv, which occurs in the refolding and shields the tryptophan residue from the aqueous environment. The small increase of the tryptophan fluorescence in the burst phase in the refolding from pH 4.0 may arise from a change in the ionization state of the protein caused by the pH change. The apparent difference in the burst phase fluorescence change between the two refolding reactions is thus attributed to a difference in the fluorescence intensity between the collapsed state and the intermediate populated at the beginning of refolding from pH 4.0.

The burst phase is followed by rapid decreases in the fluorescence intensity, which are analyzed with two exponentials with rate constants of 10.4 s^{-1} and 1.74 s^{-1} as a result of the detailed analysis in the

Figure 7. Kinetic refolding curves of GFPuv monitored by chromophore fluorescence excited at 395 nm (a), and tryptophan fluorescence excited at 295 nm (b) and (c). The reactions were initiated by pH jumps from pH 4.0 (black continuous line) and pH 2.0 (black dotted line) to pH 7.5 for (a) and (b), and from pH 2.0 to pH 4.0 for (c). The inset in (a) shows the refolding curve within 5 s. The red lines show the theoretical curves that best fit the experimental data. The best-fit values of the rate constants and amplitudes are given in Table 2. The open circle, cross, and open triangle show the fluorescence intensities of the native state at pH 7.5, the acid-denatured state at pH 2.0, and the intermediate state at pH 4.0, respectively.

Table 2. Kinetic parameters obtained by fitting of refolding curves of GFPuv from pH 2.0 to pH 7.5, from pH 4.0 to pH 7.5, and from pH 2.0 to pH 4.0, as measured by chromophore and tryptophan fluorescence at 25 °C

			Rate constant k (s^{-1}) and relative amplitude A (%)				
		Burst	1st	2nd	3rd	4th	5th
Chromophore fluorescence	pH 2.0→pH 7.5	k		2.31±0.03	0.203±0.0004	0.0311±0.0001	0.0077±0.0001
		A		−4.16±0.03	40.4±0.07	53.3±0.13	10.5±0.16
	pH 4.0→pH 7.5	k		2.31±0.03	0.203±0.000	0.0311±0.0001	0.0077±0.0001
		A		−2.67±0.03	47.2±0.06	43.4±0.13	12.0±0.15
Tryptophan fluorescence	pH 2.0→pH 7.5	k	10.4±0.3	1.74±0.13	0.124±0.011	0.0172±0.0009	0.0017±0.0007
		A −134	82.9±1.7	29.4±1.7	19.6±1.1	76.5±1.7	21.9±1.7
	pH 4.0→pH 7.5	k	10.4±0.3	1.74±0.13	0.124±0.011	0.0172±0.0009	0.0017±0.0007
		A −35.3	1.15±1.14	21.3±1.1	27.0±1.1	67.3±2.3	27.6±1.7
	pH 2.0→pH 4.0	k	0.826±0.023				
		A −23.5	52.9±0.5				

The relative amplitudes for the denatured state and the native state were 0% and 100%, respectively. The kinetic traces recorded at the same final pH value using the same probe (tryptophan or chromophore fluorescence) were fitted using global fitting methods, where the rate constants (k_i) were the global parameters.

present study, although we previously reported that this fluorescence decrease was fitted with a single exponential.[8] The amplitude of the faster (the first) phase (10.4 s^{-1}) in refolding from pH 2.0 was 82.9%, but that in refolding from pH 4.0 was almost disappeared (1.15%). The amplitude (21.3%) of the slower (the second) phase (1.74 s^{-1}) in refolding from pH 4.0 was smaller than that (29.4%) in refolding from pH 2.0. Therefore, these results suggest that the kinetic folding intermediates formed in these rapid fluorescence-decreasing phases may correspond to the equilibrium unfolding intermediate accumulated at pH 4.0 (see Discussion).

After the rapid fluorescence-decreasing phases, the slow fluorescence-decreasing phases (the third, forth and fifth phases) were observed, and these phases correspond to either the formation of the native structure from the intermediate or to slow prolyl isomerizations in the intermediate states. These third, forth and fifth phases were identical between the refolding reactions started from pH 2.0 and pH 4.0.

Kinetic refolding reaction from the acid-denatured state (pH 2.0) to the equilibrium intermediate (pH 4.0)

We also investigated the refolding kinetics from pH 2.0 to pH 4.0 as monitored by tryptophan fluorescence (Figure 7(c)), from which we can compare the kinetics of the formation of the equilibrium intermediate at pH 4.0 with the kinetics of that of the folding intermediates at pH 7.5. The fluorescence increases in the burst phase (−23.3%) and decreases rapidly with a rate constant of 0.842 s^{-1}, and then there are no subsequent slower fluorescence changes. The rate constant of 0.842 s^{-1} was slower than the rate constants (10.4 s^{-1} and 1.74 s^{-1}) of the formation of the kinetic folding intermediates in the refolding at pH 7.5. However, this phase may correspond to the formation of the intermediate, because it is very likely that the lower stability of the GFPuv intermediate at pH 4.0 than at pH 7.5 decelerates the formation of the intermediate.

Discussion

We studied the acid denaturation of GFPuv by chromophore fluorescence, tryptophan fluorescence and SAXS, and detected an equilibrium unfolding intermediate populated at pH 4.0. We also studied the kinetic refolding reactions of GFPuv induced by pH jumps from pH 2.0 (denatured) to pH 7.5 (native), from pH 4.0 (intermediate) to pH 7.5 (native), and from pH 2.0 (denatured) to pH 4.0 (intermediate). These refolding reactions were monitored by chromophore fluorescence and tryptophan fluorescence. At least two kinetic folding intermediates were detected in the refolding from pH 2.0 to pH 7.5, and these intermediates were shown to be the equivalent of, or at least closely related to, the equilibrium intermediate populated at pH 4.0 (see below). Furthermore, when the kinetic refolding reaction was initiated from pH 4.0 and monitored by tryptophan fluorescence, the first observable phase in the refolding from pH 2.0 disappeared. Because the equilibrium population of the D state is virtually absent at pH 4.0 (the fraction of D is estimated to be 0.007 from the parameter values given in Table 1), this suggests that the first observable phase may correspond to a refolding process from the D state to the intermediate (see below).

It is interesting to note that the observation of the two kinetic folding intermediates, equivalent to the pH 4 equilibrium unfolding intermediate, is very analogous to the observation previously reported for apomyoglobin. Apomyoglobin exhibits partly folded intermediates, equivalent to the equilibrium molten globule accumulated at pH 4.[22] However, there are also remarkable differences between GFPuv and apomyoglobin. Apomyoglobin is a typical α-helical protein, and hence has a very different backbone topology from GFPuv, a typical β-sheet protein. The folding rate is also very different between the two proteins, and the rate constant is 100-fold faster in apomyoglobin.[32] The ionizable groups responsible for the transition from the native state to the intermediate are also

different between apomyoglobin and GFPuv (see below).

In the following, we further discuss the characteristics of the equilibrium unfolding intermediate of GFPuv populated at pH 4.0, the kinetic refolding of the protein from the acid-denatured state, and the relationship between the equilibrium intermediate and the kinetic folding intermediates. Finally we compare the folding mechanism of GFPuv with those of the other non-two-state globular proteins, and also identify the ionizable groups responsible for the acid transitions of GFPuv.

Characteristics of the equilibrium intermediate

The SAXS and fluorescence measurements of the pH 4 intermediate of GFPuv indicated that the intermediate state has the characteristics of the molten globule state, in which a hydrophobic core around Trp57 is organized. The wavelength of the tryptophan fluorescence peak of the intermediate is close to that in the native state, so that it is significantly blue-shifted compared with that of the denatured state. The fluorescence intensity of the intermediate is significantly higher than that of the native state. These findings indicate that Trp57 in the pH 4 intermediate is buried in a hydrophobic environment but that the fluorescence of the tryptophan residue is not sufficiently quenched by the GFPuv chromophore. Because the chromophore shows no fluorescence, the specific tertiary structure in the vicinity of the chromophore is not yet organized in the intermediate. From the $P(r)$ function of the SAXS pattern of GFPuv at pH 4.0, the intermediate is compact and globular but more expanded than the native state. The shoulder of the $P(r)$ function of the intermediate shown in Figure 5 is very similar to that observed in the salt-induced molten globule intermediate of apomyoglobin.[28] The R_g value of the intermediate calculated from the $P(r)$ function was 32.3 Å, 40% larger than that of the native state, and hence this was larger than the value (10% to 30% larger than that of the native state) expected for a typical molten globule state of other globular proteins.[18]

Kinetic refolding of GFPuv from the acid-denatured state

From the present as well as the previous results, the kinetic refolding of GFPuv from the acid-denatured state can be divided into at least six kinetic phases:[8] (1) the burst phase (>200 s^{-1}), with the formation of the burst phase intermediate I_b (non-specific collapse); (2) the first phase (10 s^{-1}), with the formation of the first intermediate I_1; (3) the second phase (2 s^{-1}), with the formation of the second intermediate I_2; (4) the third phase (0.2 s^{-1}), with the formation of the native structure through a faster track of parallel folding pathways; (5) the forth phase (0.03 s^{-1}), with the peptidyl-prolyl *cis-trans* isomerization and the formation of the native structure through a slower track of parallel folding pathways; and (6) the fifth phase (0.008 s^{-1}), with the peptidyl-prolyl *cis-trans* isomerization.

The rapid decrease in tryptophan fluorescence after the burst phase was previously reported to be a single exponential, but the more precise analysis in the present study has shown that it is divided into the two phases, the first and the second, that have rate constants of 10.4 s^{-1} and 1.74 s^{-1}, respectively. The coincidence in the rate constant between the second phase in the tryptophan kinetics and the lag phase in the kinetics monitored by the GFPuv chromophore further supports the identification of the first and second phases, and the observation of the second phase as the lag phase in the chromophore fluorescence that monitors the final native structure provides evidence that the intermediate I_2 must be an on-pathway intermediate. The first phase (10.4 s^{-1}), which was accompanied by the formation of the first intermediate I_1, was newly detected in the present study. I_1 may have a compact structure, since the fluorescence of Trp57 was highly quenched by the GFPuv chromophore. It is assumed that I_1 is formed before the on-pathway intermediate (I_2), so that the folding scheme of GFPuv from the acid-denatured state (D) is given by:

$$D \rightarrow I_b \rightarrow I_1 \rightarrow I_2 \rightarrow N. \qquad \text{Scheme 2}$$

This scheme is the simplest, and comparison of the observed kinetics of refolding from different pH values, pH 2.0 and pH 4.0, supports this simplest scheme (see below). Here, for simplicity, the slow prolyl isomerizations that occur in the denatured and intermediate states are ignored, and only the major track (faster track) of parallel pathways of refolding is considered. A more detailed reaction scheme that involves the slow prolyl isomerizations and the parallel pathways of refolding of GFPuv has been shown in a previous report.[8]

Relationship between the pH 4 equilibrium intermediate and the kinetic folding intermediates

From the comparison between the refolding kinetics induced by pH jumps from pH 2.0 to pH 7.5 and from pH 4.0 to pH 7.5, we can prove the relationship between the pH 4 equilibrium intermediate and the kinetic folding intermediates. Because the denatured (D) state is eventually absent at equilibrium at pH 4.0, the disappearance of the first (I_b to I_1) phase (10.4 s^{-1}) monitored by tryptophan fluorescence in the refolding from pH 4.0 is consistent with Scheme 2. On the other hand, the second (I_1 to I_2) and third (I_2 to N) phases and the other slower phases were observed in the refolding from pH 4.0 as well as in the refolding from pH 2.0. The amplitude of the second phase observed in the refolding from pH 4.0 was, however, about 70% of the amplitude of the same phase observed in the refolding from pH 2.0 (Table 2). A similar behavior was observed in the refolding kinetics monitored by the GFPuv chromophore, and

the negative amplitude of the second phase (lag phase) in the refolding from pH 4.0 was 65% of the amplitude of the same phase in the refolding from pH 2.0. These results thus clearly demonstrate that the pH 4 equilibrium intermediate of GFPuv is composed of the two intermediate species, I_1 (65–70%) and I_2 (30–35%).

Although the equilibrium measurements by the tryptophan and the chromophore fluorescence have detected two intermediates, the pH 4 intermediate (I) and the native-like intermediate (N′) (Scheme 1), N′ is essentially the native state, different from either I_1 or I_2. N′ exhibits 50% to 60% of the native chromophore fluorescence (see Figure 4(c)), while the chromophore fluorescence is absent in both I_1 and I_2. The tryptophan fluorescence decreases during the refolding processes from I_1 and I_2, while the fluorescence increases from N′ to N (Figure 4(b)).

When the refolding of GFPuv was induced by a pH jump from pH 2.0 to pH 4.0 and monitored by tryptophan fluorescence, we observed the formation of only the intermediates (Figure 7(c)), and we did not observe the formation of the native state. The observed kinetics were single exponential with a rate constant a little smaller than the rate constant of the second phase observed at pH 7.5, and this may be due to some pH dependence of the rate constant of formation of the intermediate.

Comparison of the folding mechanism of GFPuv with those of other proteins

The present study supports a hierarchical model of protein folding, in which the intermediate with the characteristics of the molten globule state plays an important role in acquiring the final native structure efficiently. It has been shown by the stopped-flow CD, the stopped-flow fluorescence, the stopped-flow SAXS, and the pulsed-hydrogen exchange NMR techniques that a number of proteins, including α-lactalbumin, apomyoglobin, and ribonuclease HI, exhibit kinetic folding intermediates that resemble the equilibrium molten globule intermediate formed under a mildly denaturing condition.[17–24] A number of other proteins also exhibit the molten globule intermediate at a mildly acidic pH (pH 4) at equilibrium, and these proteins include human stefin B,[33] acidic fibroblast growth factor,[34] and apolipoprotein E4.[35]

Among these proteins, apomyoglobin shows a folding mechanism similar to that of GFPuv described above,[22] although the backbone topologies of the two proteins are very different from each other. GFPuv is composed mainly of β-sheets, while apomyoglobin is composed of α-helices. Apomyoglobin is known to show an equilibrium unfolding intermediate with the characteristics of the molten globule state at pH 4, and the intermediate is very similar to the kinetic intermediate at an early stage of the refolding, as pulsed-hydrogen exchange NMR studies have clearly shown. Apomyoglobin folds through two molten-globule-like intermediates in a hierarchical manner, and GFPuv also folds through the two intermediates (I_1 and I_2) (Scheme 2). The intermediates of apomyoglobin have a heterogeneous structure in which the native-like structure is localized in a region of the A, G, and H-helices. Similarly, the intermediate structure of GFPuv is heterogeneous, in which one side of the molecule including Trp57 is more organized than the other side of the molecule.[8]

There are, however, remarkable differences in the formation of the intermediate and the folding behavior between apomyoglobin and GFPuv. The accumulation of the intermediate of apomyoglobin at pH 4.0 is known to be caused by a single buried histidine (His24) that has an abnormally low pK_a value in the native state.[36] In contrast, the accumulation of the pH 4 intermediate of GFPuv is caused by five abnormal carboxyl residues (Table 1) (see below). The rate constants of the formation of the molten-globule-like intermediate (2.3 s^{-1}) and the subsequent formation of the native structure of GFPuv (0.20 s^{-1}) are 100-fold slower than the corresponding rate constants of apomyoglobin.[32] A previous study has shown that the rate constant for the formation of the intermediate and for the subsequent formation of the native structure is highly correlated with structure-based parameters that represent the backbone topology and/or the arrangement of sub-structures of the native three-dimensional structure.[14,37] GFPuv is a large single domain protein (27 kDa) with a complicated backbone topology composed mainly of β-sheets, and therefore the above structure-based parameters are much larger than those of apomyoglobin. This may result in the remarkably slower rate constant for the formation of the intermediate and the subsequent formation of the native structure in GFPuv.

Ionizable groups responsible for the acid-induced transitions

The transition from the native state to the pH 4 intermediate (the N′I transition) of GFPuv is associated with five carboxyl residues that have abnormally low pK_a values in the native state (Table 1). The transition from the pH 4 intermediate to the acid-denatured state (the ID transition) is also associated with another set of five carboxyl residues that have abnormally low pK_a values in the native and the intermediate states. Therefore, there must be at least ten abnormal carboxyl residues in native GFPuv. We thus closely examined the X-ray structure of GFPuv (PDB code: 1b9c)[15] and found a number of hydrogen-bonding salt bridges between carboxylate side-chains of glutamyl and aspartyl residues and positively charged side-chains of basic amino acid residues (His, Lys, and Arg). These salt bridge pairs include Asp21-Lys126, Asp82–Lys85, Asp102–Lys101, Glu111–Arg109, Glu115–Arg122, Asp180–Lys166, Asp197–His81, Asp210–Lys45, and Glu213–(Lys45/Arg215). In all these pairs, an oxygen atom of the carboxylate is within a hydrogen-bonding distance from a side-chain nitrogen

atom of the basic residue. In addition, there is a buried carboxylate (Glu222) that is included by a hydrogen-bond network within the GFPuv molecule[15] and this carboxylate may also be abnormal. As a whole, we have thus found at least ten candidate residues for the abnormal carboxyls.

The transition from the native state to the native-like intermediate (the NN′ transition) of GFPuv was found to be caused by an abnormal histidine (Table 1). In fact, GFPuv has histidine residues (His148, His169, and His181) that are buried in a hydrophilic side of the β-barrel. In particular, His148 and His 181 may have abnormally low pK_a values compared with those in bulk water, and hence can contribute to the accumulation of the N′ state. The N_ε atom of the side-chain of His148 is hydrogen-bonded with the peptide NH of Arg168 that is involved in β-strand 8, and that of His181 is hydrogen-bonded with the side-chain OH of Thr62 that is involved in the central helix.

Materials and Methods

Protein expression and purification

The GFPuv variant (F99S/M153T/V163A) of wild-type green fluorescent protein was overexpressed in *Escherichia coli* and was purified from the soluble extract of *E. coli* cells by a known procedure.[16]

Fluorescence spectral measurements

All equilibrium spectral measurements of GFPuv were carried out at 25.0 °C. All the solutions used in the equilibrium experiments contained 1 mM DTT. Protein concentration was determined by UV absorption using a molar absorption coefficient of ε (280 nm) = 2.06×10^4 $M^{-1}cm^{-1}$ of GFPuv,[16] which corresponds to an extinction coefficient of $E^{0.1\%}_{1cm} = 0.77$ considering the molecular mass (2.67×10^4) of the protein.

Fluorescence measurements were carried out on a spectrofluorometer (FP-777; Jasco, Tokyo, Japan). Tryptophan fluorescence spectra were measured as follows. The protein solution was excited at 295 nm, and the spectral bandwidth was set at 3.0 nm for both excitation and emission. The unfolding transition curve monitored by chromophore fluorescence was measured by the fluorescence intensity at 508 nm excited at 395 nm. The spectral bandwidth was set at 1.5 nm for both excitation and emission. The protein stock solutions were prepared in 10 mM Tris (pH 7.5). The unfolding reactions were initiated by mixing the stock solution with an appropriate unfolding buffer depending on the final pH values of the reaction with a mixing ratio of 1:1. The unfolding buffers were 20 mM Tris, phosphate, and sodium acetate for the measurement of the final pH of 7.5, pH 7–6, and pH 6–3, respectively.

SAXS measurements

The SAXS experiments were performed at beamline 15A of the Photon Factory at the High Energy Accelerator Research Organization, Tsukuba, Japan.[38] The experimental details and the analysis of the scattering data were the same as described.[24] Scattering patterns were recorded by a CCD-based X-ray detector, which consisted by a beryllium–windowed X-ray image intensifier (Be-XRII) (V5445P-MOD; Hamamatsu Photonics, Tokyo, Japan), an optical lens, a CCD image sensor, and a data acquisition system (C7300; Hamamatsu Photonics), as described.[24,39,40] The buffer solutions used for the sample preparations were the same as those described above for the fluorescence spectral measurements. Pair distribution functions, *P(r)*, were calculated by an indirect Fourier transform method using GNOM.[27] The values for the radius of gyration (R_g) were computed from the *P(r)* functions using GNOM. For the use of the GNOM software, we consulted the home page†.

Analysis of the transition curves and the SVD of the SAXS data

The global fitting of the three unfolding transition curves of GFPuv measured by tryptophan and chromophore flurescence (Figure 4(b) and (c)) to equations (1) and (2) was carried out using SigmaPlot for Windows Ver. 8.0 (SPSS Inc.). The SVD of the SAXS data was carried out using Microsoft Excel with a Visual Basic for Application macro.

Kinetic fluorescence measurements

All kinetic refolding measurements of GFPuv were carried out at 25.0 °C. Each solution used in the kinetic experiments contained 1 mM DTT. The kinetic refolding experiments were carried out using an SX.18MV stopped-flow apparatus (Applied Photophysics, Surrey, UK). The dead time of the apparatus was 5 ms. The protein stock solutions were prepared in HCl at pH 2.0 and 20 mM sodium acetate (pH 4.0). Refolding reactions were initiated by mixing the stock solution with an appropriate refolding buffer depending on the final pH values of the reaction with a mixing ratio of 1:1. The refolding buffers used were 40 mM Tris and 40 mM sodium acetate for the measurement of the final pH of 7.5 and pH 4.0, respectively. For the refolding measurements monitored by chromophore fluorescence, the emission was recorded using a 460 nm high-pass filter (SC-46; Fuji Photo Film, Tokyo, Japan) with an excitation wavelength of 395 nm. For the refolding measurements monitored by tryptophan fluorescence, the emission was recorded using a 350 nm band-pass filter (U-350; Hoya, Tokyo, Japan) with an excitation wavelength of 295 nm. The final protein concentrations were 0.01 mg/ml and 0.04 mg/ml for the measurements monitored by chromophore and tryptophan fluorescence, respectively.

Kinetic analysis

The kinetic data recorded at pH 7.5 were fitted by non-linear least-squares using the following equation:

$$A(t) = A(\infty) - \sum \Delta A_i e^{-K_i t}, \quad (3)$$

where $A(t)$ and $A(\infty)$ are the fluorescence intensities at time t and the infinite time, respectively; in addition, ΔA_i

† http://www.embl-hamburg.de/ExternalInfo/Research/Sax/index.html

and k_i are the amplitude and the apparent rate constant of the *i*th phase, respectively. The kinetic traces recorded at the same final pH but from different initial pH values using the same probe (tryptophan or chromophore fluorescence) were fitted using global fitting methods (SigmaPlot for Windows Ver. 8.0), where the rate constants (k_i) were the global parameters. The kinetic data recorded at pH 4.0 were fitted after the subtraction of the background fluorescence at pH 4.0, which arose from a non-negligible degradation effect.

Acknowledgements

We thank Professor Yoshiyuki Amemiya and Professor Katsuzo Wakabayashi for giving us the opportunity to use the CCD-based X-ray detector coupled with the beryllium-windowed X-ray image intensifier. This work was supported by a Grant-in-Aid for Scientific Research on Priority Areas (no. 15076201) and a Grant-in-Aid for Scientific Research (B) (no.17370052) from the Ministry of Education, Culture, Science, Sports and Technology (MEXT) of Japan. It was performed under the approval of the Photon Factory (proposal number 2004G384).

References

1. Ormo, M., Cubitt, A. B., Kallio, K., Gross, L. A., Tsien, R. Y. & Remington, S. J. (1996). Crystal structure of the *Aequorea victoria* green fluorescent protein. *Science*, **273**, 1392–1395.
2. Yang, F., Moss, L. G. & Phillips, G. N., Jr (1996). The molecular structure of green fluorescent protein. *Nature Biotechnol.* **14**, 1246–1251.
3. Heim, R., Prasher, D. C. & Tsien, R. Y. (1994). Wavelength mutations and posttranslational autoxidation of green fluorescent protein. *Proc. Natl Acad. Sci. USA*, **91**, 12501–12504.
4. Reid, B. G. & Flynn, G. C. (1997). Chromophore formation in green fluorescent protein. *Biochemistry*, **36**, 6786–6791.
5. Cubitt, A. B., Heim, R., Adams, S. R., Boyd, A. E., Gross, L. A. & Tsien, R. Y. (1995). Understanding, improving and using green fluorescent proteins. *Trends Biochem. Sci.* **373**, 448–455.
6. Bokman, S. H. & Ward, W. W. (1981). Renaturation of Aequorea gree-fluorescent protein. *Biochem. Biophys. Res. Commun.* **101**, 1372–1380.
7. Ward, W. W. & Bokman, S. H. (1982). Reversible denaturation of Aequorea green-fluorescent protein: physical separation and characterization of the renatured protein. *Biochemistry*, **21**, 4535–4540.
8. Enoki, S., Saeki, K., Maki, K. & Kuwajima, K. (2004). Acid denaturation and refolding of green fluorescent protein. *Biochemistry*, **43**, 14238–14248.
9. Weissman, J. S., Rye, H. S., Fenton, W. A., Beechem, J. M. & Horwich, A. L. (1996). Characterization of the active intermediate of a GroEL-GroES-mediated protein folding reaction. *Cell*, **84**, 481–490.
10. Makino, Y., Amada, K., Taguchi, H. & Yoshida, M. (1997). Chaperonin-mediated folding of green fluorescent protein. *J. Biol. Chem.* **272**, 12468–12474.
11. Martin, J. (2002). Requirement for GroEL/GroES-dependent protein folding under nonpermissive conditions of macromolecular crowding. *Biochemistry*, **41**, 5050–5055.
12. Ueno, T., Taguchi, H., Tadakuma, H., Yoshida, M. & Funatsu, T. (2004). GroEL mediates protein folding with a two successive timer mechanism. *Mol. Cell*, **14**, 423–434.
13. Tsien, R. Y. (1998). The green fluorescent protein. *Annu. Rev. Biochem.* **67**, 509–544.
14. Kamagata, K., Arai, M. & Kuwajima, K. (2004). Unification of the folding mechanisms of non-two-state and two-state proteins. *J. Mol. Biol.* **339**, 951–965.
15. Battistutta, R., Negro, A. & Zanotti, G. (2000). Crystal structure and refolding properties of the mutant F99S/M153T/V163A of the green fluorescent protein. *Proteins: Struct. Funct. Genet.* **41**, 429–437.
16. Fukuda, H., Arai, M. & Kuwajima, K. (2000). Folding of green fluorescent protein and the Cycle3 mutant. *Biochemistry*, **39**, 12025–12032.
17. Kuwajima, K. (1989). The molten globule state as a clue for understanding the folding and cooperativity of globular-protein structure. *Proteins: Struct. Funct. Genet.* **6**, 87–103.
18. Arai, M. & Kuwajima, K. (2000). Role of the molten globule state in protein folding. *Advan. Protein Chem.* **53**, 209–282.
19. Forge, V., Wijesinha, R. T., Balbach, J., Brew, K., Robinson, C. V., Redfield, C. & Dobson, C. M. (1999). Rapid collapse and slow structural reorganisation during the refolding of bovine α-lactalbumin. *J. Mol. Biol.* **288**, 673–688.
20. Baldwin, R. L. (1993). Pulsed H/D-exchange studies of folding intermediates. *Curr. Opin. Struct. Biol.* **3**, 84–91.
21. Raschke, T. M. & Marqusee, S. (1997). The kinetic folding intermediate of ribonuclease H resembles the acid molten globule and partially unfolded molecules detected under native conditions. *Nature Struct. Biol.* **4**, 298–304.
22. Wright, P. E. & Baldwin, R. L. (2000). The folding process of apomyoglobin. In *Mechanism of Protein Folding* (Pain, R. H., ed), 2nd edit., pp. 309–329, Oxford University Press, Oxford.
23. Semisotnov, G. V., Kihara, H., Kotova, N. V., Kimura, K., Amemiya, Y., Wakabayashi, K. *et al.* (1996). Protein globularization during folding. A study by synchrotron small-angle X-ray scattering. *J. Mol. Biol.* **262**, 559–574.
24. Arai, M., Ito, K., Inobe, T., Nakao, M., Maki, K., Kamagata, K. *et al.* (2002). Fast compaction of α-lactalbumin during folding studied by stopped-flow X-ray scattering. *J. Mol. Biol.* **321**, 121–132.
25. Lakowicz, J. R. (1983). Protein fluorescence. In *Principles of fluorescence spectroscopy.* 2nd edit., pp. 445–486, Plenum Press, New York.
26. Tanford, C. (1970). Protein denaturation C. Part, Theoretical models for the mechanism of denaturation. *Advan. Protein Chem.* **24**, 1–95.
27. Svergun, D. I. (1992). Determination of the regularization parameter in indirect-transform methods using perceptual criteria. *J. Appl. Crystallog.* **25**, 495–503.
28. Kataoka, M. & Goto, Y. (1996). X-ray solution scattering studies of protein folding. *Fold. Design*, **1**, R107–R114.
29. Kohn, J. E., Millett, I. S., Jacob, J., Zagrovic, B., Dillon, T. M., Cingel, N. *et al.* (2004). Random-coil behavior and the dimensions of chemically unfolded proteins. *Proc. Natl Acad. Sci. USA*, **43**, 12491–12496.
30. Henry, E. R. & Hofrichter, J. (1992). Singular value

decomposition: application to analysis of experimental data. *Methods Enzymol.* **210**, 129–192.
31. Doniach, S. (2001). Changes in biomolecular conformation seen by small angle X-ray scattering. *Chem. Rev.* **101**, 1763–1778.
32. Uzawa, T., Akiyama, S., Kimura, T., Takahashi, S., Ishimori, K., Morishima, I. & Fujisawa, T. (2004). Collapse and search dynamics of apomyoglobin folding revealed by submillisecond observations of alpha-helical content and compactness. *Proc. Natl Acad. Sci. USA*, **101**, 1171–1176.
33. Zerovnik, E., Jerala, R., Kroon-Zitko, L., Turk, V. & Lohner, K. (1997). Characterization of the equilibrium intermediates in acid denaturation of human stefin B. *Eur. J. Biochem.* **245**, 364–372.
34. Sanz, J. M. & Gimenez-Gallego, G. (1997). A partly folded state of acidic fibroblast growth factor at low pH. *Eur. J. Biochem.* **246**, 328–335.
35. Morrow, J. A., Hatters, D. M., Lu, B., Hochtl, P., Oberg, K. A., Rupp, B. & Weisgraber, K. H. (2002). Apolipoprotein E4 forms a molten globule. A potential basis for its association with disease. *J. Biol. Chem.* **277**, 50380–50385.
36. Geierstanger, B., Jamin, M., Volkman, B. F. & Baldwin, R. L. (1998). Protonation behavior of histidine 24 and histidine 119 in forming the pH 4 folding intermediate of apomyoglobin. *Biochemistry*, **37**, 4254–4265.
37. Kamagata, K. & Kuwajima, K. (2006). Surprisingly high correlation between early and late stages in non-two-state protein folding. *J. Mol. Biol.* **357**, 1647–1654.
38. Amemiya, Y., Wakabayashi, K., Hamanaka, T., Wakabayashi, T., Matsushima, T. & Hashizume, H. (1983). Design of a small-angle X-ray diffractometer using synchrotron radiation at the phton factory. *Nucl. Instrum. Methods Phys. Res.* **208**, 471–477.
39. Ito, K., Kamikubo, H., Yagi, N. & Amemiya, Y. (2005). Correction method and software for image distortion and nonuniform response in charge-coupled device-based X-ray detectors utilizing X-ray image intensifier. *Jpn. J. Appl. Phys.* **44**, 8684.
40. Amemiya, Y., Ito, K., Yagi, N., Asano, Y., Wakabayashi, K., Ueki, T. & Endo, T. (1995). Large-aperture TV detector with a beryllium-windowed image intensifier for X-ray diffraction. *Rev. Sci. Instrum.* **66**, 2290–2294.

Edited by C. R. Matthews

(Received 4 March 2006; received in revised form 25 June 2006; accepted 5 July 2006)
Available online 4 August 2006